RESEARCH ARTICLE

Key Points:
- Methane $\delta^{13}C$ isotopic signatures have been measured in the tropics for wetland, rice, ruminant, and biomass burning
- Wetlands, rice, and ruminants are depleted in ^{13}C, but it is difficult to distinguish between them; biomass burning values are enriched in ^{13}C
- Isotopic measurements are essential in determining the causes of methane growth

Supporting Information:
- Supporting Information S1
- Data Set S1

Correspondence to:
R. Brownlow and E. G. Nisbet,
rebecca.brownlow.2009@live.rhul.ac.uk;
e.nisbet@es.rhul.ac.uk

Isotopic Ratios of Tropical Methane Emissions by Atmospheric Measurement

R. Brownlow[1] , D. Lowry[1] , R. E. Fisher[1] , J. L. France[2] , M. Lanoisellé[1] , B. White[1], M. J. Wooster[3,4], T. Zhang[3,4], and E. G. Nisbet[1]

[1]Department of Earth Sciences, Royal Holloway, University of London, Egham, UK, [2]Centre for Oceanic and Atmospheric Sciences, School of Environmental Sciences, University of East Anglia, Norwich, UK, [3]Department of Geography, King's College London, Strand, UK, [4]NERC National Center for Earth Observation, Leicester, UK

Abstract Tropical methane sources are an important part of the global methane budget and include natural wetlands, rice agriculture, biomass burning, ruminants, fossil fuels, and waste. $\delta^{13}C_{CH4}$ can provide strong constraints on methane source apportionment. For example, tropical wetlands in this study give $\delta^{13}C_{CH4}$ values between $-61.5 \pm 2.9‰$ and $-53.0 \pm 0.4‰$ and in general are more enriched in ^{13}C than temperate and boreal wetlands. However, thus far, relatively few measurements of $\delta^{13}C_{CH4}$ in methane-enriched air have been made in the tropics. In this study samples have been collected from tropical wetland, rice, ruminant, and biomass burning emissions to the atmosphere. Regional isotopic signatures vary greatly as different processes and source material affect methane signatures. Measurements were made to determine bulk source inputs to the atmosphere, rather than to study individual processes. These measurements provide inputs for regional methane budget models, to constrain emissions with better source apportionment.

Plain Language Summary Tropical methane sources are an important part of the global methane budget and include natural wetlands, rice agriculture, biomass burning, ruminants, fossil fuels, and waste. Carbon isotopes in methane can provide strong constraints on methane source apportionment. However, thus far, relatively few measurements of carbon isotopes in methane-enriched air have been made in the tropics. In this study samples have been collected from tropical wetland, rice, ruminant, and biomass burning emissions to atmosphere. Regional isotopic signatures vary greatly as different processes and source material affect methane signatures. Measurements were made to determine bulk source inputs to the atmosphere, rather than to study individual processes, to provide inputs for regional methane budget models, and to constrain emissions with better source apportionment.

1. Introduction

In 2007 a sustained growth of atmospheric methane began, with the global methane mole fraction increasing by 5.7 ± 1.2 ppb yr^{-1} from 2007 to 2013. Growth rate was higher in 2014 at 12.6 ± 0.5 ppb, in 2015 at 9.8 ± 0.7 ppb, and in 2016 at 8.5 ± 0.7 ppb (Dlugokencky, 2017). The growth was particularly strong in the tropics (Nisbet et al., 2016), with atmospheric inversions suggesting 359 Tg yr^{-1} of methane between 2003 and 2012, approximately 64% of global methane emissions (Saunois et al., 2016). The largest natural source is tropical wetlands (Mitsch et al., 2009; Saunois et al., 2016) with other tropical sources including rice agriculture, natural and anthropogenic biomass burning, ruminants (such as cattle, water buffalo, and sheep), fossil fuels and waste. However, the factors driving methane growth remain controversial (Dalsøren et al., 2016; Dlugokencky et al., 2009; Hausmann et al., 2016; Nisbet et al., 2016; Rigby et al., 2017; Schaefer et al., 2016; Schwietzke et al., 2016; Turner et al., 2017).

To help resolve the causes of the rise in methane, modeling of the methane isotopic budget can place strong constraints on sources and sinks; however, modeling is hampered by the lack of detailed knowledge of isotopic ratios of tropical sources. Here we provide isotopic measurements of methane from these different sources and use these to provide constraints on methane source apportionment.

Emissions estimates of methane from "bottom-up" (estimated fluxes of individual processes) and "top-down" (fluxes inferred from atmospheric measurements) methodologies differ greatly. Bottom-up approaches tend to give higher global methane estimates than top-down. One possible reason for this is that larger individual emissions are inferred from natural sources (Kirschke et al., 2013; Nisbet et al., 2014; Saunois et al., 2016).

Isotopic measurements can help constrain these budgets, but more such measurements are required, especially from tropical regions. Methane flux and isotopic measurements are predominantly made in developed countries, and there are far fewer measurements in tropical areas (Bousquet et al., 2006; Dlugokencky et al., 2011).

Different processes of methane production and consumption have characteristic $^{13}C/^{12}C$ ratios ($\delta^{13}C_{CH4}$) (e.g., Dlugokencky et al., 2011), and so this ratio is useful in helping identify changing sources and sinks. Relative to background ambient air, which has a $\delta^{13}C_{CH4}$ of approximately $-47‰$ (Allan et al., 2001; Nisbet et al., 2016), emissions can be either enriched or depleted in ^{13}C. Atmospheric sinks impose a kinetic isotope effect (KIE) of about 4 to 6‰ on isotopic ratios as reaction with OH occurs at a faster rate for $^{12}CH_4$ compared to $^{13}CH_4$. The global isotopic bulk methane source averages around $-53‰$. Sink fractionation means background ambient air at present has a signature between -47.4 and $-47.2‰$ (Allan et al., 2001; Nisbet et al., 2016).

Biogenic sources are depleted in the heavier isotope (e.g., an Arctic wetland may give a signature of $-71‰$ (Fisher et al., 2017)), while thermogenic/pyrogenic sources are enriched in ^{13}C (e.g., biomass burning of C_4 plants at -10 to $-20‰$ (Dlugokencky et al., 2011)). Schwietzke et al. (2016) compiled a database of isotopic methane source signatures, but very few tropical nonfossil fuel sources were included.

Since the 2007 sustained methane growth began, $\delta^{13}C_{CH4}$ has shifted globally to more negative values. This contrasts with $\delta^{13}C_{CH4}$ enrichment during methane growth in the 1980s and 1990s showing that source or sink changes are different (Schaefer et al., 2016).

This may suggest an increased biogenic source either from increased agricultural emissions (Schaefer et al., 2016) or increased emissions from wetlands as a result of meteorological variations and/or changing climate (Nisbet et al., 2016). An alternative explanation may be the due to changes in the OH sink. Turner et al. (2017) suggested a decline in the OH sink which is partially offset by a decline in methane emissions. Rigby et al. (2017) also modeled variations in the OH sink and suggested that OH changes may have played a role in the methane growth rate contributing to the more depleted $\delta^{13}C_{CH4}$ signature.

Models tend to focus on methane mole fraction measurements, and either do not take into account the source types or use a very general global isotopic number for each source type (e.g., Rigby et al., 2012) without taking into account zonal variation of the sources, for example, boreal versus tropical latitudinal variation in emissions from wetlands (Fisher et al., 2017; Schwietzke et al., 2016; Zazzeri et al., 2016). Global and regional models that include methane isotopes should therefore include regional isotope signatures for better source apportionment, as regional variations (e.g., latitudinal) may be overlooked when using a single value (Fisher et al., 2017; Kirschke et al., 2013). Using isotopic source signatures together with mole fraction measurements to constrain global and regional emissions provides models with better source apportionment. This should permit better understanding of the sustained tropical methane growth and help close the gap between bottom-up and top-down emission estimates.

The new measurements of methane isotope signatures provided in the current work (section 3) have been made directly on air collected above tropical sources, as well as directly from individual ruminants or ruminant herds. Plumes also have been sampled downwind of larger sources. The aim is to improve the characterization of tropical methane source signatures, reducing uncertainties for specific regions of the tropics. Most previous studies of wetland and rice emissions have used chamber sampling (Fisher et al., 2017; Whiticar et al., 1986), which only sample isolated points in the wetland. Methanotrophy may also occur in the chambers which may further fractionate the methane emissions released to the atmosphere; however, the extent of this is unknown. Localized vegetation and microbial processes within the chamber and disturbance to the natural local microenvironment mean that an individual chamber may not fully represent the wider wetland emissions entering the atmosphere (Sriskantharajah et al., 2012). Ambient air sampled in this study is taken from open air above wetlands. This therefore represents the mixed methane inputs to the atmosphere, from which average wetland isotopic signatures for a local regional source can be assessed (Fisher et al., 2017).

1.1. Wetlands

It is estimated that tropical wetlands between 30°N and 30°S emit 126 ± 31 Tg yr^{-1} of methane (Melton et al., 2013). The term "wetland" describes a range of methane emitting ecosystems, including wet soils, swamps,

bogs, and peatlands. Rice fields are an anthropogenic source but share the same mechanisms and controls for methane emissions as natural wetlands.

In wetlands, methanogenesis can occur through two main pathways that vary with specific environments and affect the isotopic signature: Fermentation of acetate (acetotrophic methanogenesis) and reduction of CO_2 with hydrogen (hydrogenotrophic methanogenesis). Hydrogenotrophic methanogenesis produces methane with a $\delta^{13}C_{CH4}$ of −110‰ to −60‰ which is more negative than acetotrophic methanogenesis, which produces methane with a $\delta^{13}C_{CH4}$ of −60‰ to −50‰ (Whiticar et al., 1986). Partial oxidation of methane by methanotrophs may cause significant enrichment in ^{13}C in the sediment column before it is emitted to the atmosphere (Schaefer & Whiticar, 2008). Methane can exit wetland surfaces and enter the atmosphere via diffusion, ebullition, and/or plant mediated channeling. The degree of oxidation and therefore the isotopic signature depends on the pathway that the methane follows to the atmosphere. Mixing then occurs in the atmosphere, giving a more general source signature (Chanton, 2005; Chanton et al., 2005; Whiticar et al., 1986).

These different production pathways in wetlands may be influenced by temperature, vegetation type, and the water table, which is linked to the anoxia level and the availability of substrate (Saunois et al., 2016; Whiticar, 1999). Hydrological processes are a major control on tropical wetland methane emissions and may play a larger role than in higher latitudes where temperature and seasonality may be a more important factor (Bousquet et al., 2011; Ringeval et al., 2010). In the rice paddies, water management and rice type affect methane production along with significant in situ methanotrophy (Conrad, 2002). Methane is predominantly released by diffusive transport through the rice plant (Saunois et al., 2016).

1.2. Biomass Burning

Intense dry season anthropogenic biomass burning occurs throughout much of the tropics and subtropics, resulting in significant methane emissions (Saunois et al., 2016). Contributing sources include seasonal C_4 grassland burning, especially in African savannahs, C_3 forest fires, including those related to deforestation, shifting cultivation, wildfires (anthropogenic or naturally ignited), and use of fuel wood, for cooking, heating, and industry (Chanton et al., 2000; Crutzen & Andreae, 1990). Tropical biomass biomass burning typically shows very strong seasonality, and in some areas strong interannual variations due to meteorological shifts and/or climate anomalies (e.g., Wooster et al., 2012). Tropical biomass burning emissions of methane are estimated to be 13.6–34.5 Tg yr^{-1} (Kirschke et al., 2013), though there are significant increases in some years/locations, e.g., El Niño related droughts increasing the availability of combustible fuel (e.g., Huijnen et al., 2016).

Factors affecting the amount of methane emitted by tropical burning include the amount of fuel burned, its moisture content, and its type, the latter affecting the methane emissions factor (the amount of methane released per kilogram of fuel burned (Andreae & Merlet, 2001)). The photosynthetic pathway of carbon capture is important. C_3 plants (e.g., woody trees or most temperate crops) and C_4 plants (dominating many tropical grasslands) have different $\delta^{13}C_{CH4}$ signatures, reflected in the isotopic signatures of the methane emitted. C_4 vegetation preconcentrates CO_2 and thus is ^{13}C enriched compared to C_3 plants. In contrast, methane from burning C_3 vegetation is more depleted in ^{13}C. Isotopic ratios also appear to depend on fire conditions. For example, fires in a particular ecosystem that are flaming involve per unit area rates of heat release and fuel consumption typically far higher than when smoldering, with significantly lower methane emissions factors (e.g., Wooster et al., 2011), but with smoke appearing generally more enriched in ^{13}C (Chanton et al., 2000). However, the different fuels preferentially accessed by the fires during natural flaming and smoldering activity, and the amount of moisture present can complicate interpretations of in situ collected smoke samples in relation to the isotopic signatures.

1.3. Ruminants

It is possible that agricultural emissions (rice and ruminants) may have increased in the tropics recently (Schaefer et al., 2016). However, few ruminant isotopic signatures have been measured, especially in the tropics (Schwietzke et al., 2016), so expanding the methane isotope data set for ruminant emissions is highly valuable.

Around 26% of global land area is dedicated to grazing (Ripple et al., 2013). The African and South American tropics and India host large populations of domesticated cattle. In 2014 Africa was estimated to have 312 million cattle, South America 352 million cattle, and India 187 million cattle, around 21%, 24%, and 13%, respectively (Food and Agricultural Organisation of the United Nations (FAO), 2016). Deforestation occurs widely in part in the tropics to make way for livestock, helping to drive fire emissions (Ripple et al., 2013). In 2014 cattle contributed to 73.0% of global ruminant methane emissions and water buffalo contributed 10.8% as assessed in inventory studies (FAO, 2016). Water buffalo are found mainly in Southern Asia, with the majority of the population located in India, Pakistan, and China, so they are a significant methane contributor in these regions (FAO, 2016).

Ruminants may be either native or domesticated and consume plants that are digested through enteric fermentation. They are a significant source of anthropogenic methane with ~94% of animal emissions being from domesticated animals (Ripple et al., 2013; Thorpe, 2008). In less economically developed countries, many of which are in the tropics, livestock populations have increased in response to human population growth. Greenhouse gas emissions from livestock are estimated to have risen by 117% in less economically developed countries from 1961 to 2010 (Caro et al., 2014).

Nearly all of the methane emitted from ruminants is produced in the rumen then exhaled (Hook et al., 2010). Domesticated ruminants were estimated (bottom-up) to produce around 99 Tg of methane in 2014 (FAO, 2016). Factors influencing methane emissions vary with geographical location, C_3 or C_4 plant composition and quality of the feed, processing of feed and the breed of the animal (Hook et al., 2010). Tropical ruminants may graze on C_4 savannah grasslands or consume C_3 or C_4 based feed including C_4 maize, sugar cane tops, millet, sorghum crop waste, or C_3 trees and bushes (Bakrie et al., 1996).

1.4. Other Sources

Fossil fuel emissions of methane occur in coal, oil, and gas extraction and use. Coal emits methane during extraction, crushing, processing, and burning, and from abandoned mines. Methane is flared in oil extraction. Major emissions come from natural gas extraction, flaring, processing, distribution, and use (Dlugokencky et al., 2011). Fossil methane is mainly thermogenic and comes from the transformation of organic matter into fossil fuels over a geological period of time (Ciais et al., 2013). Globally fossil fuel emissions contribute between 114 and 133 Tg CH_4 yr^{-1} to the atmosphere (Saunois et al., 2016). Tropical gas source regions include Southeast Asia, Bolivia, Venezuela, Nigeria, Qatar, and Algeria, and India is the major coal source region.

Waste sources include the decomposition of biodegradable municipal solid waste in landfills, animal waste, and human waste (Dlugokencky et al., 2011). These combined sources produce between 67 and 90 Tg CH_4 yr^{-1} (Ciais et al., 2013). In many tropical countries the gases produced from biodegradation in landfill receive no treatment and are directly released into the atmosphere (Wangyao et al., 2010).

Other natural sources such as termites (biogenic) or geological sources (such as oceanic seeps or mud volcanoes) also contribute to the methane budget (Saunois et al., 2016).

1.5. Sinks

Oxidation by OH radicals, predominantly in the troposphere, is the main sink of atmospheric methane (90% of the global sink), particularly in the tropics due to the combination of relatively intense solar radiation, high temperatures, and high moisture (Kirschke et al., 2013).

Removal of methane by OH imposes a kinetic isotope shift of 4 to 6‰ on the remaining atmospheric methane (Allan et al., 2007). Oxidation by methanotrophic bacteria in soils also enriches $\delta^{13}C_{CH4}$ and contributes to a methane loss of about 30 Tg yr^{-1} (Ciais et al., 2013; Dlugokencky et al., 2011). Karst systems also may act as a net sink of atmospheric methane through microbial oxidation (Mattey et al., 2013). Other sinks include Cl and Br radicals in the marine boundary layer, Cl, and oxygen radicals in the stratosphere. The KIE from the Cl sink enriches atmospheric methane by 2.6 ± 1.2‰ (Allan et al., 2007).

1.6. Tropical Source Values

Table 1 shows literature-derived values for tropical sources. Fossil fuel sources, including in the tropics, are well defined in the literature (Schwietzke et al., 2016; Sherwood et al., 2016); however, wetlands, agriculture (rice and ruminants), waste, and biomass burning are less well studied.

Table 1
Summary of Methane Sources From Literature, Focussing on the Tropics if the Data Is Available

Source		$\delta^{13}C_{CH4}$ (‰)	Reference
Tropical wetlands	Sampling method		
Mangroves: Florida Everglades	Glass dome or plexiglas Pyramid	−70.1 ± 1.8	Chanton et al. (1988)
Swamps: Southern Thailand	Inverted Funnel	−66.1 ± 5.1	Nakagawa et al. (2002)
Floodplain: Amazon	Flask samples at ground Level	−63.7 ± 6	Tyler et al. (1987)
Swamps: Nyahururu, Kenya	Stainless steel ring-bag enclosure	−61.7 ± 0.5	Tyler et al. (1988)
Everglades: Florida	Flask surface air samples	−55 ± 3	Stevens and Engelkemeir (1988)
Floodplain: Amazon	Inverted funnel and flux chamber	−53 ± 8	Quay et al. (1988)
Swamp: North Florida	Chamber	−52.7 ± 6.1	Happell et al. (1994)
Rice agriculture	Sampling method		
Rice paddies: Japan	Chamber	−70 to −57	Tyler et al. (1994)
Rice paddy: Kenya	Stainless steel ring-bag enclosure	−63 to −57	Tyler et al. (1988)
Rice paddies: India	Chamber	−57.2 to −54.3	Rao et al. (2008)
Rice paddies: peat soils Southern Thailand	Gas bubbles trapped in inverted funnel	−56.5 ± 4.6	Nakagawa et al. (2002)
Rice paddies: mineral soils Southern Thailand	Gas bubbles trapped in inverted funnel	−51.5 ± 7.1	Nakagawa et al. (2002)
Termites			
Kenya		−61.6 ± 8	Tyler et al. (1988)
Ruminants			
C_3 diet: Germany		−74 to −60	Stevens and Engelkemeir (1988),
C_4 diet: Germany		−55 to −50	Levin et al. (1993), and Klevenhusen et al. (2010)
Biomass burning	Fire type		
C_3 plants: primary forest slash fires, Brazil	Smoldering	−26.87 ± 0.2 and -30.61 ± 0.2	Snover et al. (2000)
	Flaming	−29.1 ± 0.2	
C_3 plants: African woodland	Smoldering	−30.4 ± 1.3	Chanton et al. (2000)
	Flaming	−30.1 ± 1	
C_3 plants: agricultural grass field		−24 to −32	Stevens and Engelkemeir (1988)
C_4 plants: Zambian savanna	Smoldering	−26.1 ± 6	Chanton et al. (2000)
	Flaming	−16.6 ± 2	
C_4 plants: brown grass, Brazil		−12.45 ± 0.2	Snover et al. (2000)
Waste (Europe)		−55 ± 5	Levin et al. (1993) and Bergamaschi et al. (1998)
Fossil fuels			
Coal: Brazil		−53.2 ± 1.4	Levandowski (2009)
Coal: sub-Saharan Africa		−52.2 ± 3.8	Ward et al. (2004)
Conventional gas: India		−54.2 ± 12.6	Pande et al. (2011)
Conventional gas: Indonesia		−44.3 ± 11.6	Satyana et al. (2007)
Conventional gas: Brazil		−42.2 ± 6.2	Prinzhofer et al. (2010) and Prinzhofer et al. (2000)
Conventional gas: Thailand		−40.6 ± 4.2	Giggenbach (1997) and Jenden (1988)

Note. Note a lack of ruminant and waste tropical studies, so more general values are used.

2. Methodology

2.1. Sampling Methods

Air samples were collected in 3 L Tedlar bags (SKC Ltd) using a battery operated pump at each of the sites (Figure 1 and Table S1). The bags were filled at varying distances downwind and upwind from the sources to allow for a range of methane mole fractions. Wetland and rice paddy samples were taken at heights between 5 cm and 3 m above the source. Ruminant samples were taken between a few centimeters to 2–3 m away from the head of the animal. Biomass burning samples were mostly taken between 30 cm and a few meters away from the fires, with some further afield in downwind plumes. The sampled Chinese fires were burning agricultural wastes, the Malaysian fires were burning local waste, and the Chisipite Vlei, Zimbabwean fire was uncontrolled. Some sampled Zimbabwean fires were controlled burns. The Chinese and Malaysian samples were taken throughout flaming and smoldering stages. The airline was flushed before the bag was attached and opened to remove any residual air from the previous sample.

Figure 1. Sampling sites showing a wide coverage of the tropics.

2.2. Laboratory Analysis

The Tedlar bag samples were analyzed in the Greenhouse Gas Laboratory at Royal Holloway University of London (RHUL). A Picarro 1301 cavity ring down spectrometer (CRDS) measured the mole fraction of methane calibrated to the NOAA 2004A scale. The Picarro CRDS measures linearly up to 20 ppm, so methane samples with higher mole fractions must be diluted with nitrogen before analysis. The 3 L Tedlar bags were analyzed for 240 s with the last 120 s of measurements being used to calculate the mean mole fraction. If the bags had less air they were analyzed for 120 s with the final 60 s being used for the mean mole fraction calculation. The precision of the instrument for methane is ±0.2 ppb (600 s) for the standards and ±0.4 ppb for the bag samples due to the much shorter averaging time.

Continuous-flow gas chromatography/isotope ratio mass spectrometry (CF-GC/IRMS) using a modified Trace Gas-Isoprime system (Fisher et al., 2006) allows for precise $\delta^{13}C_{CH4}$ analysis of methane with repeatability of 0.05‰. A minimum of 0.5 L of air sample is retained for the $\delta^{13}C_{CH4}$ isotopic analysis (Fisher et al., 2017). The isotope ratios are given in δ notation on the VPDB (Vienna Pee Dee Belemnite) scale. An internal secondary standard is analyzed at least three times the beginning of each day, or until the measurements are stable, and after every two samples to allow correction for instrumental drift throughout the day. Samples are measured in triplicate with an additional measurement analysis if the first three are not within 0.1‰. If the recorded mole fraction in the sample was above 7 ppm, it was diluted to be in the linear and dynamic range of the mass spectrometer for isotopic analysis (Fisher et al., 2006).

2.3. Isotopic Source Signatures

Keeling plot regression (Keeling, 1958; Pataki et al., 2003; Zazzeri et al., 2015) is used to identify the isotopic source signature of the methane in the samples. The $\delta^{13}C_{CH4}$ is plotted against the inverse of the methane mole fraction, then linear regression is used to calculate the isotopic source signature responsible for the excess over background (the y intercept—equation (1)). Orthogonal regression is used to take into account both errors on the x and y axes (Akritas & Bershady, 1996).

$$\delta^{13}C_a = c_b \left(\delta^{13}C_b - \delta^{13}C_s\right) \times (1/c_a) + \delta^{13}C_s \qquad (1)$$

C_a is the atmospheric mole fraction of a gas and C_b is the background atmospheric mole fraction. $\delta^{13}C_a$ is the measured isotopic composition, $\delta^{13}C_b$ is the background isotopic composition, and $\delta^{13}C_s$ is the source isotopic composition.

The Bivariate Correlated Errors and intrinsic Scatter (BCES) program (available at http://www.astro.wisc.edu/~mab/archive/stats/stats.html) accommodates for the errors in x and y in each sample. BCES regression has been used to find the uncertainty of the Keeling plot intercept and therefore the error in the $\delta^{13}C$ source signature (Akritas & Bershady, 1996; Zazzeri et al., 2015).

3. Results

Results are given in Table 2 with corresponding Keeling plots in the supporting information.

3.1. Wetland and Rice Sources

The newly studied tropical wetland sources give methane emissions with $\delta^{13}C_{CH4}$ between -61.5 ± 2.9‰ and -53.0 ± 0.4‰. This is within or near the range of other tropical wetland or swamp studies. Table 1 shows sources from tropical wetland sources between -66 and -52‰.

Tropical wetlands are in general more enriched in ^{13}C than temperate and boreal wetlands; for example, Fisher et al. (2017) gives a value of -71 ± 1‰ for European Arctic wetland emissions. The enrichment of ^{13}C in tropical wetlands may be due to thicker oxic zones in the sediments or water column compared to northern wetlands. Oxidation effects leave the methane more enriched in ^{13}C. The difference of northern and tropical wetlands may also be due to differences in methanogenic communities, temperature differences, and precursor plant material in the northern wetlands being C_3 compared to the tropics where C_4 plants are more abundant (Chanton, 2005; Fisher et al., 2017; Nakagawa et al., 2002).

The Hong Kong rice values are -58.7 ± 0.4‰ and -58.9 ± 0.4‰ taken during rice growth in July. Literature values given in Table 1 show rice paddies in tropical areas to range between -70 to -51‰. The more depleted values of -70‰ for Japanese rice paddies were found to be seasonal (Tyler et al., 1994); however, other studies have found little variation between the growth stages of the rice (Tyler et al., 1988). Nakagawa et al. (2002) gives a value of -63 ± 5‰ for temperate rice paddies. More general rice paddy signatures are given by Dlugokencky et al. (2011) with a value of -62 ± 3‰ and Schaefer et al. (2016) with values of -59 to -65‰. The new results are representative of ambient air rather than using chamber measurements or similar techniques, which look at small scale processes (Fisher et al., 2017).

The literature values for wetlands and rice agriculture are predominantly chamber studies or using an inverted funnel and are more variable than atmospheric samples that have been mixed (Fisher et al., 2017). These new results show that simple atmospheric grab sampling gives results consistent with averages from chamber studies and are more representative values for regional modeling.

The Costa Rican mangrove samples, from a saline environment, are more depleted in ^{13}C than the other sites between -77.7 ± 0.2‰ to -70.1 ± 2.4‰. This is comparable to mangroves in the Florida Everglades with a signature of -70 ± 2‰ (Chanton et al., 1988). These differences may be due to more acetoclastic methanogenesis occurring in the freshwater tropics, while hydrogenotrophic methanogenesis is the more dominant process in marine sediment environments such as the Costa Rican mangroves (Whiticar et al., 1986). In comparison the Hong Kong reed, mangrove, and marshes at Mai Po, an environment with both freshwater and brackish marine components, give -54.6 ± 0.7‰. This is comparable to the Florida everglades, Stevens and Engelkemeir (1988) with a value of -55 ± 3‰ and Happell et al. (1994) with a value of -52.7 ± 6.1‰.

3.2. Ruminant Sources

Feral water buffalo from Hong Kong with a predominantly C_3 diet gave a $\delta^{13}C_{CH4}$ emission value of -63.3 ± 0.4‰ and domesticated Hong Kong cows gave -70.5 ± 0.7‰. Farmed cattle in Zimbabwe emitted methane between -56.9 ± 0.4‰ and -52.5 ± 0.6‰ for a predominantly C_4 diet (see Table S2). Ruminants which digest C_3 plants shown in Table 1 have signatures between -74 and -60‰ attributed to them in atmospheric studies (Dlugokencky et al., 2011; Schaefer et al., 2016). Values of ruminants which digest C_4 plants (Table 1) have signatures between -55 and -50‰ attributed to them in atmospheric studies (Dlugokencky et al., 2011; Schaefer & Whiticar, 2008).

3.3. Biomass Burning

The C_3 plant biomass burning methane $\delta^{13}C_{CH4}$ signatures from China and Malaysia lie between -33.4 ± 0.6‰ and -28.5 ± 0.4‰. These are similar to African woodlands that gave a value of -30‰ (Chanton et al., 2000) and an agricultural grass field and dried tree branches with values of -24 to -32‰ (Stevens & Engelkemeir, 1988). The C_4 plant results of -18.7 ± 0.3‰ and -15.9 ± 1.3‰ from Zimbabwe are comparable to Zambian savanna burns which give a mean value of -16.6‰ at a flaming stage of burning (Chanton et al., 2000).

Table 2
Methane $\delta^{13}C$ Source Signature Results From This Study

Source and sample date	Sample site	Description	Source signature (‰)	No. of samples
Wetland				
June 2016	Pui O, Hong Kong	Marsh (C_3 and C_4)	−52.3 ± 0.7	6
May 2014	Papyrus swamp, Uganda	Papyrus swamp (C_4)	−53.0 ± 0.4	9
February 2016	Palo Verde National Park, Costa Rica	Coastal floodplain freshwater marsh (C_3 and C_4)	−53.3 ± 1.7	5
May 2014	Edge of Lake Victoria, Uganda	Freshwater wetland: papyrus (mostly C_4)	−58.7 ± 4.1	6
February 2014	Lake Titicaca, Bolivia	Freshwater wetland (C_3)	−59.7 ± 1.0	11
June 2016	Yi O, Hong Kong	Marsh (C_3 and C_4)	−60.2 ± 0.4	12
August 2015	Danum Valley Borneo	Forest wetland (C_3)	−61.5 ± 2.9	11
December 2014	Tor Doone, South Africa	Freshwater wetland (C_3)	−61.5 ± 0.1	11
June 2016	Mai Po, Hong Kong	Reed (C_4), mangroves (C_3), and marshes	−54.6 ± 0.7	9
January 2016	Costa Rica mangroves, Sierpe, and Puerto Jimenez	Mangroves (C_3)	−70.1 ± 2.4 to −77.7 ± 0.2	4 and 4
Rice Paddies				
June 2016	Hong Kong Rice, Yi O	Rice (C_3)	−58.7 ± 0.4	16
June 2016	Hong Kong Rice, Hok Tau	Rice wetland (C_3)	−58.9 ± 0.4	11
Enteric Fermentation				
C_4				
July 2016	Zimbabwe Lobels cows	Eating C_4	−52.5 ± 0.6	9
June 2016	Zimbabwe Dom cows	Eating mostly C_4	−56.8 ± 0.5	11
July 2016	Zimbabwe Tavistock cows	Eating C_4 and C_3	−56.9 ± 0.4	9
C_3				
June 2016	Hong Kong water buffalo	Eating mostly C_3	−63.3 ± 0.4	5
June 2016	Hong Kong cows	Eating C3	−70.5 ± 0.7	12
Biomass Burning				
C_3				
June 2014	China	Wheat and oil plant crop residue	−28.5 ± 0.4 to −33.4 ± 0.6	5 and 5
January 2014	Bachok, Malaysia	Mango wood	−32.8 ± 0.2 to −30.3 ± 0.2	3 and 3
C_4				
July 1998	Zimbabwe	Grass	−16.3 ± 0.1 to −18.8 ± 0.3	3 and 3
August 2016	Chisipite Vlei, Zimbabwe	Grass	−15.9 ± 1.3	6

Notes. The Keeling plots for these are given in supporting information Figures S1–S4. The uncertainties (1σ) given take into account both variables ($\delta^{13}C_{CH4}$ and CH_4 mole fraction) (described in section 2).

There is little $\delta^{13}C_{CH4}$ fractionation during biomass burning due to the high combustion temperature; however, if the biomass is damp, the combustion temperature may decrease. The main factor affecting the source signature is the plant type being C_3 or C_4 (Bréas et al., 2001; Quay et al., 1991) and these results confirm the need to separate these values in models. The limited data sets show no difference between flaming and smoldering stages of the burning in terms of isotopic signatures.

4. Summary

Figure 2 shows that the source values measured in this study and literature values generally compare well. The types of mangroves should be taken into account as saline, and freshwater/brackish conditions have different signatures; however, these coastal saltwater environments have been shown to produce relatively little methane (Matthews & Fung, 1987; Bartlett et al., 1985). This is also the first study of $\delta^{13}C_{CH4}$ emissions from tropical ruminants with measurements made in the field of ambient air close to the animals to give a well-mixed signature. Overall, the wetlands, mangroves, rice sources, and ruminants are depleted in ^{13}C but it is difficult to distinguish between them. The biomass burning values are enriched in ^{13}C.

In the equatorial and wet savannah tropics of South America, Africa and South East Asia emissions are likely to be from primarily wetland sources with mean top-down estimates being 40 Tg yr^{-1}, 20 Tg yr^{-1}, and 27 Tg yr^{-1}, respectively (Saunois et al., 2016). In contrast, emissions from China, India and Northern Africa are likely to be predominantly from agricultural sources, as well as fossil fuel emissions. Mean top-down estimates for the agriculture and waste category in these regions are 27 Tg yr^{-1}, 25 Tg yr^{-1} and 12 Tg yr^{-1}, respectively (Saunois et al., 2016). Agriculture is also an important source for South East Asia with mean top-down estimates being 24 Tg yr^{-1} (Saunois et al., 2016).
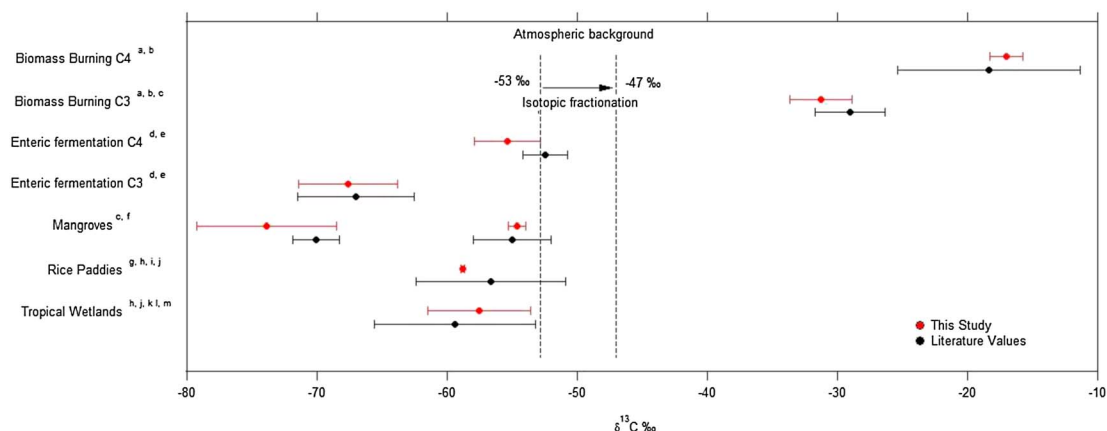
Figure 2. Tropical $\delta^{13}C_{CH4}$ source value ranges taken from both this study only (red) and literature values (black): a: Chanton et al. (2000), b: Snover et al. (2000), c: Stevens and Engelkemeir (1988), d: Klevenhusen et al. (2010) (nontropical study), e: Levin et al. (1993) (nontropical study), f: Chanton et al. (1988), g: Tyler et al. (1994), h: Tyler et al. (1988), i: Rao et al. (2008), j: Nakagawa et al. (2002), k: Tyler et al. (1987), l: Quay et al. (1988), and m: Happell et al. (1994). The uncertainties for this study are shown as standard deviations of the average signatures. The error bars on the literature values show the variability within the literature. The dashed lines show the global average $\delta^{13}C_{CH4}$ source signature, between -53.6 and -53.4‰ with the sink fractionation ‰ leaving the residual ambient background air with a signature close to -47‰ (Allan et al., 2001; Nisbet et al., 2016).

Biogenic wetland and rice emissions and pyrogenic biomass burning emissions have strong seasonality. This seasonality is especially strong in the African savannah. For example, Northern Hemisphere African burning primarily occurs between December and March, shifting the average continental signal in this region toward less negative isotopic values. This period coincides with the most negative (biogenic) values in the Southern Hemisphere Africa region during the wet season (Roberts et al., 2009). For this reason seasonal bulk isotopic sources and emissions inventories would be useful to further constrain methane sources especially in regions such as tropical Africa and South America.

Biogenic sources (wetlands, ruminants, waste, etc.) have indistinguishable $\delta^{13}C_{CH4}$ signatures in the tropical regions. Waste $\delta^{13}C_{CH4}$ values in the tropics may also be different from managed landfill sites in Europe that many studies are based on. More detailed land use maps in the tropics may help in quantifying the inputs of different sources. More regular isotopic measurements are needed throughout the tropics to take into account measurement gaps and seasonality.

Isotope measurements provide strong constraints on methane source apportionment; however, it is important to take into account variation of isotopic signatures when modeling such as the latitudinal variation of wetlands and the regional biogenic sources. The measurements in this study are more representative of source emissions as a whole, rather than individual processes, and can be included in regional models to constrain the methane emissions with better source apportionment.

4.1. Possible Mechanisms for the Renewed Growth and the Usefulness of Isotopes

Turner et al. (2017) have argued that the large overlap in isotopic signatures at process level makes it difficult to use isotopes to draw conclusions about methane source changes. However, within a region at larger integrated scales well-defined (bulk) source signatures for main source categories can be determined. As isotope source signatures differ in the Northern and Southern Hemispheres as well as regionally, it is important to take variants (for example, C_3 and C_4 ratios in cattle feed or biomass burning and wetland types over a wide region) into account when using $\delta^{13}C_{CH4}$. Chamber studies show a wide range of isotope source signatures due to various small scale processes; however, in this study, well-mixed grab samples of air above wetlands have been taken which are more representative of overall wetland signatures. In conclusion, regional signatures should be applied in atmospheric model studies rather than process level source signatures.

Turner et al. (2017) have also suggested that the most likely solution to the renewed methane growth is due to a decline in the OH sink which is partially offset by a decline in methane emissions. Variations in the OH sink and suggested OH changes may have played a role in the methane growth rate contributing to the more depleted $\delta^{13}C_{CH4}$ signature (Rigby et al., 2017). A 1% change of OH in the troposphere is equivalent to around 5 Tg CH$_4$ yr^{-1} emission change (globally about 2 ppb change in methane mole

fraction). A decrease of the OH sink would also mean $\delta^{13}C_{CH4}$ values would become more depleted (Nisbet et al., 2016). OH abundance is poorly understood, and Nisbet et al. (2016) consider OH changes unlikely to be the cause of recent changes in atmospheric $\delta^{13}C_{CH4}$ as rapid large shifts are needed which cannot be explained by destruction of methane alone. There are also no obvious reasons why OH may have varied. Globally, OH change is thought to be well buffered, varying less than 1% during 2006–2008, while other trace gas measurements oxidized by OH suggest that the 2007 methane increase may only partially be explained by OH (Montzka et al., 2011).

Thus, although sinks may have changed, Schaefer et al. (2016) and Nisbet et al. (2016) interpreted the renewed growth and shift toward more depleted $\delta^{13}C_{CH4}$ as primarily driven by increased biogenic sources. It has been suggested that these biogenic sources may be from either increased agricultural emissions (Schaefer et al., 2016) or increased emissions from wetlands as a result of meteorological changes, such as strong positive rainfall anomalies (Nisbet et al., 2016).

This study has contributed to measurements of $\delta^{13}C_{CH4}$ isotopic signatures from different tropical sources. Emissions of methane from the tropics are predominantly wetland emissions with $\delta^{13}C_{CH4}$ source signatures from this study between −61.5 ± 2.9‰ and −53.0 ± 0.4‰, rice around −58‰, and ruminants with signatures between −52.5 ± 0.6‰ and −70.5 ± 0.7‰ which are all depleted. If these emissions are increasing, then it could explain the $\delta^{13}C_{CH4}$ isotopic shift to more depleted values.

The ongoing debate assigning the renewed methane growth and isotopic shift to biogenic sources or changes in the sink processes remains unresolved. More measurements, particularly in areas with seasonal source emissions, are needed to improve constrains on tropical sources and therefore better explain the causes of sustained methane growth in the tropics. Only when there is a much better understanding of the regional differences and seasonal changes in isotopic signatures will the root cause of the global isotopic trends be understood.

References

Akritas, M. G., & Bershady, M. A. (1996). Linear regression for astronomical data with measurement errors and intrinsic scatter. *The Astrophysical Journal*, *470*, 706.

Allan, W., Manning, M. R., Lassey, K. R., Lowe, D. C., & Gomez, A. J. (2001). Modeling the variation of $\delta^{13}C$ in atmospheric methane: Phase ellipses and the kinetic isotope effect. *Global Biogeochemical Cycles*, *15*, 467–481. https://doi.org/10.1029/2000GB001282

Allan, W., Struthers, H., & Lowe, D. C. (2007). Methane carbon isotope effects caused by atomic chlorine in the marine boundary layer: Global model results compared with Southern Hemisphere measurements. *Journal of Geophysical Research*, *112*, D04306. https://doi.org/10.1029/2006JD007369

Andreae, M. O., & Merlet, P. (2001). Emission of trace gases and aerosols from biomass burning. *Global Biogeochemical Cycles*, *15*, 955–966. https://doi.org/10.1029/2000GB001382

Bakrie, B., Hogan, J., Liang, J. B., Tareque, A. M. M., & Upadhyay, R. C. (1996). Ruminant nutrition and production in the tropics and subtropics, ACIAR Monograph No. 36.

Bartlett, K. B., Harriss, R. C., & Sebacher, D. I. (1985). Methane flux form coastal salt marshes. *Journal of Geophysical Research*, *90*, 5710–5720. https://doi.org/10.1029/JD090iD03p05710

Bergamaschi, P., Lubina, C., Königstedt, R., Fischer, H., Veltkamp, A. C., & Zwaagstra, O. (1998). Stable isotopic signatures ($\delta^{13}C$, δD) of methane from European landfill sites. *Journal of Geophysical Research*, *103*, 8251–8265. https://doi.org/10.1029/98JD00105

Bousquet, P., Ciais, P., Miller, J. B., Dlugokencky, E. J., Hauglustaine, D. A., Prigent, C., … White, J. (2006). Contribution of anthropogenic and natural sources to atmospheric methane variability. *Nature*, *443*(7110), 439–443. https://doi.org/10.1038/nature05132

Bousquet, P., Ringeval, B., Pison, I., Dlugokencky, E. J., Brunke, E.-G., Carouge, C., … Ciais, P. (2011). Source attribution of the changes in atmospheric methane for 2006–2008. *Atmospheric Chemistry and Physics*, *11*, 3689–3700. https://doi.org/10.5194/acp-11-3689-2011

Bréas, O., Guillou, C., Reniero, F., & Wada, E. (2001). The Global Methane Cycle: Isotopes and Mixing Ratios, Sources and Sinks. *Isotopes in Environmental and Health Studies*, *37*(4), 257–379. https://doi.org/10.1080/10256010108033302

Caro, D., Davis, S. J., Bastianoni, S., & Caldeira, K. (2014). Global and regional trends in greenhouse gas emissions from livestock. *Climatic Change*, *126*, 203–216.

Chanton, J. P. (2005). The effect of gas transport on the isotope signature of methane in wetlands. *Organic Geochemistry*, *36*, 753–768.

Chanton, J. P., Pauly, G. G., Martens, C. S., Blair, N. E., & Dacey, J. W. H. (1988). Carbon isotopic composition of methane in Florida Everglades soils and fractionation during its transport to the troposphere. *Global Biogeochemical Cycles*, *2*, 245–252. https://doi.org/10.1029/GB002i003p00245

Chanton, J. P., Rutkowski, C. M., Schwartz, C. C., Ward, D. E., & Boring, L. (2000). Factors influencing the stable carbon isotopic signature of methane from combustion and biomass burning. *Journal of Geophysical Research*, *105*, 1867–1877. https://doi.org/10.1029/1999JD900090

Chanton, J., Chaser, L., Glasser, P., & Siegel, D. (2005). Carbon and hydrogen isotopic effects in microbial methane from terrestrial environments. In L. B. Flanagan, J. R. Ehleringer, & D. E. Pataki (Eds.), *Stable Isotopes and Biosphere Atmosphere Interactions* (pp. 85–105). Oxford: Elsevier.

Ciais, P., Sabine, C., Bala, G., Bopp, L., Brovkin, V., Canadell, J., … Thornton, P. (2013). Carbon and other biogeochemical cycles, in: Climate change 2013: The physical science basis. In T. F. Stocker et al. (Eds.), *Contribution of Working Group I to the Fifth Assessment Report of the Intergovernmental Panel on Climate Change* (pp. 465–570). Cambridge, UK and New York: Cambridge Univ. Press.

Conrad, R. (2002). Control of microbial methane production in wetland rice fields. *Nutrient Cycling in Agroecosystems*, *64*, 59–69.

Crutzen, P. J., & Andreae, M. O. (1990). Biomass burning in the tropics: Impact on atmospheric chemistry and biogeochemical cycles. *Science*, *250*, 1669–1678.

Dalsøren, S. B., Myhre, C. L., Myhre, G., Gomez-pelaez, A. J., Søvde, O. A., Isaksen, I. S. A., … Harth, C. M. (2016). Atmospheric methane evolution the last 40 years. *Atmospheric Chemistry and Physics*, *16*, 3099–3126.

Dlugokencky, E. J. (2017). NOAA/ESRL. [Available at www.esrl.noaa.gov/gmd/ccgg/trends_ch4/.]

Dlugokencky, E. J., Bruhwiler, L., White, J. W. C., Emmons, L. K., Novelli, P. C., Montzka, S. A., … Gatti, L. V. (2009). Observational constraints on recent increases in the atmospheric CH_4 burden. *Geophysical Research Letters*, *36*, L18803. https://doi.org/10.1029/2009GL039780

Dlugokencky, E. J., Nisbet, E. G., Fisher, R., & Lowry, D. (2011). Global atmospheric methane: Budget, changes and dangers. *Philosophical Transactions. Series A, Mathematical, Physical, and Engineering Sciences*, *369*(1943), 2058–2072. https://doi.org/10.1098/rsta.2010.0341

Fisher, R. E., Lowry, D., Wilkin, O., Sriskantharajah, S., & Nisbet, E. G. (2006). High precision, automated stable isotope analysis of atmospheric methane and carbon dioxide using continuous-flow isotope-ratio mass spectrometry. *Rapid Communications in Mass Spectrometry*, *20*(2), 200–208. https://doi.org/10.1002/rcm.2300

Fisher, R. E., France, J. L., Lowry, D., Lanoisellé, M., Brownlow, R., Pyle, J. A., … Nisbet, E. G. (2017). Measurement of the ^{13}C isotopic signature of methane emissions from Northern European wetlands. *Global Biogeochemical Cycles*, *31*, 605–623. https://doi.org/10.1002/2016GB005504

Food and Agricultural Organisation of the United Nations (FAO) (2016). FAOSTAT emissions database, agriculture, enteric fermentation. [Available at http://faostat3.fao.org/download/G1/GE/E] (Accessed 15 Oct 2016).

Giggenbach, W. F. (1997). Relative importance of thermodynamic and kinetic processes in governing the chemical and isotopic composition of carbon gases in high-heatflow sedimentary basins. *Geochimica et Cosmochimica Acta*, *61*, 3763–3785.

Happell, J. D., Chanton, J. P., & Showers, W. (1994). The influence of methane oxidation on the stable isotopic composition of methane emitted from Florida Swamp forests. *Geochimica et Cosmochimica Acta*, *58*, 4377–4388.

Hausmann, P., Sussmann, R., & Smale, D. (2016). Contribution of oil and natural gas production to renewed increase in atmospheric methane (2007–2014): Top–down estimate from ethane and methane column observations. *Atmospheric Chemistry and Physics*, *16*, 3227–3244.

Hook, S. E., Wright, A.-D. G., & McBride, B. W. (2010). Methanogens: Methane producers of the rumen and mitigation strategies. *Archaea*. https://doi.org/10.1155/2010/945785

Huijnen, V., Wooster, M. J., Kaiser, J. W., Gaveau, D. L. A., Flemming, J., Parrington, M., … van Weele, M. (2016). Fire carbon emissions over maritime southeast Asia in 2015 largest since 1997. *Scientific Reports*, *6*, 26886. https://doi.org/10.1038/srep26886

Jenden, P. D. (1988). *Analysis of Gases in the Earth's Crust* (pp. 571). Chicago: Gas Research Institute.

Keeling, C. D. (1958). The concentration and isotopic abundances of atmospheric carbon dioxide in rural areas. *Geochimica et Cosmochimica Acta*, *13*, 322–334.

Kirschke, S., Bousquet, P., Ciais, P., Saunois, M., Canadell, J. G., Dlugokencky, E. J., … Zeng, G. (2013). Three decades of global methane sources and sinks. *Nature Geoscience*, *6*(10), 813–823. https://doi.org/10.1038/ngeo1955

Klevenhusen, F., Bernasconi, S. M., Kreuzer, M., & Soliva, C. R. (2010). Experimental validation of the Intergovernmental Panel on Climate Change default values for ruminant-derived methane and its carbon-isotope signature. *Animal Production Science*, *50*(3), 159. https://doi.org/10.1071/AN09112

Levandowski J. H. (2009). *Petrologia e Geoquimica Das Camadas De Carvao E Sua Relacao Com Gas Natural Determinado No Poco*. (pp. 92). Porto Alegre, Brazil: Dissertation, Universidade Federal do Rio Grande do Sul.

Levin, I., Bergamaschi, P., Dörr, H., & Trapp, D. (1993). Stable isotopic signature of methane from major sources in Germany. *Chemosphere*, *26*(1–4), 161–177. https://doi.org/10.1016/0045-6535(93)90419-6

Mattey, D. P., Fisher, R., Atkinson, T. C., Latin, J.-P., Durrell, R., Ainsworth, M., … Fairchild, I. J. (2013). Methane in underground air in Gibraltar karst. *Earth and Planetary Science Letters*, *374*, 71–80.

Matthews, E., & Fung, I. (1987). Methane emissions from natural wetlands: Global distribution, area, and environmental characteristics of sources. *Global Biogeochemical Cycles*, *1*, 61–86. https://doi.org/10.1029/GB001i001p00061

Melton, J. R., Wania, R., Hodson, E. L., Poulter, B., Ringeval, B., Spahni, R., … Kaplan, J. O. (2013). Present state of global wetland extent and wetland methane modelling: Conclusions from a model inter-comparison project (WETCHIMP). *Biogeosciences*, *10*(2), 753–788. https://doi.org/10.5194/bg-10-753-2013

Mitsch, W. J., Nahlik, A., Wolski, P., Bernal, B., Zhang, L., & Ramberg, L. (2009). Tropical wetlands: Seasonal hydrologic pulsing, carbon sequestration, and methane emissions. *Wetlands Ecology and Management*, *18*, 573–586.

Montzka, S. A., Krol, M., Dlugokencky, E., Hall, B., Jöckel, P., & Lelieveld, J. (2011). Small interannual variability of global atmospheric hydroxyl. *Science*, *331*, 67–69.

Nakagawa, F., Yoshida, N., Sugimoto, A., Wada, E., Yoshioka, T., Ueda, S., & Vijarnsorn, P. (2002). Stable isotope and radiocarbon compositions of methane emitted from tropical rice paddies and swamps in Southern Thailand. *Biogeochemistry*, *61*, 1–19.

Nisbet, E. G., Dlugokencky, E. J., & Bousquet, P. (2014). Atmospheric science. Methane on the rise—again. *Science*, *343*(6170), 493–495. https://doi.org/10.1126/science.1247828

Nisbet, E. G., Dlugokencky, E. J., Manning, M. R., Lowry, D., Fisher, R. E., France, J. L., … Ganesan, A. L. (2016). Rising atmospheric methane: 2007-14 growth and isotopic shift. *Global Biogeochemical Cycles*, *30*, 1356–1370. https://doi.org/10.1002/2016GB005406

Pande, H. C., Raina, A., Roy, V., Saxena, R. K., Singh, H., & Singh, R. R. (2011). Origin of biogenic gases in east coast basins of India. Geo-India 2011 Conference. [Available at http://www.apgindia.org/pdf/649.pdf.]

Pataki, D. E., Ehleringer, J. R., Flanagan, L. B., Yakir, D., Bowling, D. R., Still, C. J., … Berry, J. A. (2003). The application and interpretation of Keeling plots in terrestrial carbon cycle research. *Global Biogeochemical Cycles* 17(1), 1022. https://doi.org/10.1029/2001GB001850

Prinzhofer, A. A., Mello, M. R., & Takaki, T. (2000). Geochemical characterization of natural gas: A physical multivariable approach and its applications in maturity and migration estimates. *AAPG Bulletin*, *84*, 1152–1172.

Prinzhofer, A., Santos Neto, E. V., & Battani, A. (2010). Coupled use of carbon isotopes and noble gas isotopes in the Potiguar basin (Brazil): Fluids migration and mantle influence. *Marine and Petroleum Geology*, *27*, 1273–1284.

Quay, P. D., King, S. L., Lansdown, J. M., & Wilbur, O. D. (1988). Isotopic composition of methane released from wetlands: Implications for the increase in atmospheric methane. *Global Biogeochemical Cycles*, *2*, 385–397. https://doi.org/10.1029/GB002i004p00385

Quay, P. D., King, S. L., Stutsman, J., Wilbur, D. O., Steele, L. P., Fung, I., … Schmidt, F. H. (1991). Carbon Isotopic Composition of Atmospheric CH4: Fossil and biomass burning source strengths. *Global Biogeochemical Cycles*, *5*, 25–47. https://doi.org/10.1029/91GB00003

Rao, D. K., Bhattacharya, S. K., & Jani, R. A. (2008). Seasonal variations of carbon isotopic composition of methane from Indian paddy fields. *Global Biogeochemical Cycles*, *22*, GB1004. https://doi.org/10.1029/2006GB002917

Rigby, M., Manning, A. J., & Prinn, R. G. (2012). The value of high-frequency, high-precision methane isotopologue measurements for source and sink estimation. *Journal of Geophysical Research*, *117*, D12312. https://doi.org/10.1029/2011JD017384

Rigby, M., Montzka, S. A., Prinn, R. G., White, J. W. C., Young, D., O'Doherty, S., … Park, S. (2017). Role of atmospheric oxidation in recent methane growth. *Proceedings of the National Academy of Sciences*, *114*, 5373–5377.

Ringeval, B., de Noblet-Ducoudre, N., Ciais, P., Bousquet, P., Prigent, C., Papa, F., & Rossow, W. B. (2010). An attempt to quantify the impact of changes in wetland extent on methane emissions on the seasonal and interannual time scales. *Global Biogeochemical Cycles*, *24*, GB2003. https://doi.org/10.1029/2008GB003354

Ripple, W. J., Smith, P., Haberl, H., Montzka, S. A., McAlpine, C., & Boucher, D. H. (2013). Ruminants, climate change and climate policy. *Nature Climate Change*, *4*, 2–5.

Roberts, G., Wooster, M. J., & Lagoudakis, E. (2009). Annual and diurnal African biomass burning temporal dynamics. *Biogeosciences*, *6*, 849–866. https://doi.org/10.5194/bg-6-849-2009

Satyana, A. H., Marpaung, L. P., Purwaningsih, M. E., & Utama, M. K. (2007). Regional gas geochemistry of Indonesia: Genetic characterization and habitat of natural gases, Proc Indonesian Petrol Assoc. [Available at http://archives.datapages.com/data/ipa_pdf/078/078001/pdfs/IPA07-G-050.pdf.]

Saunois, M., Bousquet, P., Poulter, B., Peregon, A., Ciais, P., Canadell, J. G., … Zhu, Q. (2016). The global methane budget: 2000–2012. *Earth System Science Data Discussions*, *8*, 697–751.

Schaefer, H., & Whiticar, M. J. (2008). Potential glacial-interglacial changes in stable carbon isotope ratios of methane sources and sink fractionation. *Global Biogeochemical Cycles*, *22*, GB1001. https://doi.org/10.1029/2006GB002889

Schaefer, H., Mikaloff Fletcher, S. E., Veidt, C., Lassey, K. R., Brailsford, G. W., Bromley, T. M., … White, J. W. C. (2016). A 21st century shift from fossil-fuel to biogenic methane emissions indicated by $^{13}CH_4$. *Science*, *351*(6278). https://doi.org/10.1126/science.aad2705

Schwietzke, S., Sherwood, O. A., Bruhwiler, L. M. P., Miller, J. B., Etiope, G., Dlugokencky, E. J., … Tans, P. P. (2016). Upward revision of global fossil fuel methane emissions based on isotope database. *Nature*, *538*, 88–91.

Sherwood, O., Schwietzke, S., Arling, V. & Etiope, G. (2016). Global inventory of fossil and non-fossil methane $\delta^{13}C$ source signature measurements for improved atmospheric modeling. [Available at http://doi.org/10.15138/G37P4D.]

Snover, A. K., Quay, P. D., & Hao, W. M. (2000). The D/H content of methane emitted from biomass burning ponderosa. *Global Biogeochemical Cycles*, *14*, 11–24. https://doi.org/10.1029/1999GB900075

Sriskantharajah, S., Fisher, R. E., Lowry, D., Aalto, T., Hatakka, J., Aurela, M., … Nisbet, E. G. (2012). Stable carbon isotope signatures of methane from a Finnish subarctic wetland. *Tellus B*, *64*, 1–8.

Stevens, C. M., & Engelkemeir, A. (1988). Stable carbon isotopic composition of methane from some natural and anthropogenic sources. *Journal of Geophysical Research*, *93*, 725–733. https://doi.org/10.1029/JD093iD01p00725

Thorpe, A. (2008). Enteric fermentation and ruminant eructation: The role (and control?) of methane in the climate change debate. *Climatic Change*, *93*, 407–431.

Turner, A. J., Frankenberg, C., Wennberg, P. O., & Jacob, D. J. (2017). Ambiguity in the causes for decadal trends in atmospheric methane and hydroxyl. *Proceedings of the National Academy of Sciences*, *114*, 5367–5372.

Tyler, S. C., Blake, D. R., & Rowland, F. S. (1987). 13C / 12C Ratio in Methane From the Flooded Amazon Forest. *Journal of Geophysical Research*, *92*, 1044–1048. https://doi.org/10.1029/JD092iD01p01044

Tyler, S. C., Zimmerman, P. R., Greenberg, J. P., Westberg, C., & Darlington, J. P. E. C. (1988). Measurements and interpretation of $\delta^{13}C$ of methane from termites, rice paddies, and wetlands in Kenya. *Global Biogeochemical Cycles*, *2*, 341–355. https://doi.org/10.1029/GB002i004p00341

Tyler, S. C., Brailsford, G. W., Yagi, K., Minami, K., & Cicerone, R. J. (1994). Seasonal variations in methane flux and $\delta^{13}CH_4$ values for rice paddies in Japan and their implications. *Global Biogeochemical Cycles*, *8*, 1–12. https://doi.org/10.1029/93GB03123

Wangyao, K., Yamada, M., Endo, K., Ishigaki, T., Naruoka, T., Towprayoon, S., … Sutthasil, N. (2010). Methane generation rate constant in tropical landfill. *Joural of Sustainable Energy and Environment*, *1*, 181–184.

Ward, J. A., Slater, G. F., Moser, D. P., Lin, L.-H., Lacrampe-Couloume, G., Bonin, A. S., … Sherwood Lollar, B. (2004). Microbial hydrocarbon gases in the Witwatersrand Basin, South Africa: Implications for the deep biosphere. *Geochimica et Cosmochimica Acta*, *68*, 3239–3250.

Whiticar, M. J. (1999). Carbon and hydrogen isotope systematics of bacterial formation and oxidation of methane. *Chemical Geology*, *161*, 291–314.

Whiticar, M. J., Faber, E., & Schoell, M. (1986). Biogenic Methane Formation in Marine and Fresh-Water Environments - CO2 Reduction vs Acetate Fermentation Isotope Evidence. *Geochimica et Cosmochimica Acta*, *50*(5), 693–709. https://doi.org/10.1016/0016-7037(86)90346-7

Wooster, M. J., Freeborn, P. H., Archibald, S., Oppenheimer, C., Roberts, G. J., Smith, T. E. L., … Palumbo, I. (2011). Field determination of biomass burning emission ratios and factors via open-path FTIR spectroscopy and fire radiative power assessment: Headfire, backfire and residual smouldering combustion in African savannahs. *Atmospheric Chemistry and Physics*, *11*(22), 11,591–11,615.

Wooster, M. J., Perry, G. L. W., & Zoumas, A. (2012). Fire, drought and El Niño relationships on Borneo (Southeast Asia) in the pre-MODIS era (1980–2000). *Biogeosciences*, *9*(1), 317–340.

Zazzeri, G., Lowry, D., Fisher, R. E., France, J. L., Lanoisellé, M., & Nisbet, E. G. (2015). Plume mapping and isotopic characterisation of anthropogenic methane sources. *Atmospheric Environment*, *110*, 151–162. https://doi.org/10.1016/j.atmosenv.2015.03.029

Zazzeri, G., Lowry, D., Fisher, R. E., France, J. L., Lanoisellé, M., Kelly, B. F. J., … Nisbet, E. G. (2016). Carbon isotopic signature of coal-derived methane emissions to the atmosphere: From coalification to alteration. *Atmospheric Chemistry and Physics*, *16*, 13669–13680.